Estimating Gross Primary Productivity of a tropical forest ecosystem over north-east India using LAI and meteorological variables

Estimating Gross Primary Productivity of a tropical forest ecosystem over north-east India using LAI and meteorological variables

Pramit Kumar Deb Burman[1,*], Dipankar Sarma[2], Mathew Williams[3], Anandakumar Karipot[4], and Supriyo Chakraborty[1]

[1]Centre for Climate Change Research, Indian Institute of Tropical Meteorology, Pune - 411008, India

[2]Department of Environmental Sciences, Tezpur University, Tezpur - 784028, India

[3]School of Geosciences, University of Edinburgh, Edinburgh EH9 3FF, United Kingdom

[4]Department of Atmospheric and Space Sciences, Savitribai Phule Pune University, Pune - 411007, India

[*]Corresponding author. e-mail: pramit.cat@tropmet.res.in

Abstract

Tropical forests act as a major sink of atmospheric carbon dioxide, and store large amounts of carbon in biomass. India is a tropical country with regions of dense vegetation and high biodiversity. However due to the paucity of observations the carbon sequestration potential of these forests could not be assessed in detail so far. To address this gap several flux towers were erected over different ecosystems in India by Indian Institute of Tropical Meteorology (IITM) as part of the MetFlux India project funded by MoES (Ministry of Earth Sciences, Government of India). A 50 m tall tower was set up over a semi-evergreen moist deciduous forest named Kaziranga National Park (KNP) in north-eastern part of India which houses a significant stretch of local forest cover. Climatically this region is identified to be humid sub-tropical. Here we report first generation of the in situ meteorological observations and leaf area index (LAI) measurements from this site. LAI obtained from NASA's Moderate Resolution Imaging Spectroradiometer (MODIS) is compared with the in situ measured LAI. We use these in situ measurements have also been used to calculate the total gross photosynthesis (or gross primary productivity, GPP) of the forest using a calibrated model. LAI and GPP show prominent seasonal variation. LAI ranges between 0.75 in winter to 3.25 in summer. Annual GPP is estimated to be 2.11 kgC m^{-2} $year^{-1}$.

Keywords. Gross Primary Productivity (GPP); Leaf Area Index (LAI); Aggregated Canopy Model (ACM); Moderate Resolution Imaging Spectroradiometer (MODIS); Tropical forest; MetFlux India

1 Introduction

Fluxnet is a global network of the micro-meteorological towers (Baldocchi *et al.*, 2001) erected over multiple different ecosystems distributed over a wide latitudinal area from 77^0N to 57^0S for continuous measurement of energy, water and Greenhouse Gas (GHG) fluxes between the biosphere and the atmosphere ($https://fluxnet.ornl.gov/fluxnetdb$). Continental and regional scale networks such as AmeriFlux (Boden *et al.*, 2013), AsiaFlux (Mizoguchi *et al.*, 2009), ICOS ($https://www.icos-ri.eu/$), Ozflux (Beringer *et al.*, 2016) etc. exist as part of this broad program which archive and share the quality-controlled data for the scientific community. Main objectives of this coordinated effort are to find out the global sources and sinks of GHG and ecosystem exchange patterns of energy and water vapour, to provide data for improving the land-surface processes in the models and validate the satellite products. It also aims to find out the carbon sequestration potential of the major vegetations scattered over the globe (Baldocchi *et al.*, 2001).

Gross primary productivity (GPP) is a key ecosystem parameter for understanding carbon assimilation. GPP is the rate of photosynthetic conversion of CO_2 to organic carbon by plants per unit surface area (Chapin III *et al.*, 2006). GPP has been estimated from upscaling leaf level flux measurements (Williams *et al.*, 1996) or by analysing net ecosystem flux data (Grace *et al.*, 1996; Curtis *et al.*, 2002; Saigusa *et al.*, 2005). These estimates are used for calibrating and validating models simulations of GPP and its variation at multiple spatial and temporal scales (Coops *et al.*, 2007; Jung *et al.*, 2011; El-Masri *et al.*, 2013; Barman *et al.*, 2014). Different land-surface models have been enhanced by comparing their predicted GPP against Fluxnet

observations (Bonan, 1995; Sellers *et al.*, 1997; Bonan *et al.*, 2011; Schaefer *et al.*, 2012). Several researchers have calculated GPP using radiation parameters such as PAR (Photosynthetically Active Radiation) and LUE (Light Use Efficiency) (Garbulsky *et al.*, 2010; Wu *et al.*, 2011). Data products from different satellites such as Moderate Resolution Imaging Spectroradiometer (MODIS), Landsat etc. have also been used to predict the GPP of different biomes (Turner *et al.*, 2003; Gitelson *et al.*, 2012).

Leaf Area Index (LAI) is a dimensionless vegetation index that is a strong constraint on GPP. For a broadleaf canopy it is defined as the total one-sided leaf surface area per unit ground area (Watson, 1947). It controls radiation and precipitation interception by the canopy, microclimate within the canopy and water and CO_2 exchange between the canopy and the atmosphere. Thus it plays a crucial role in estimating GPP and is one of the primary components for process-based land-surface biogeochemical models (Bréda, 2003). There are multiple techniques to estimate LAI including satellite observation (Gower *et al.*, 1999), airborne measurements (Solberg *et al.*, 2009) and ground-based direct and indirect measurements (Jonckheere *et al.*, 2004). Several studies exist where LAI measurements conducted at various Fluxnet sites have been used for estimating GPP (Chen *et al.*, 2006; Muraoka *et al.*, 2010).

South Asia (SA) ranks among the most densely populated regions in the world. It is located in the tropical belt and the terrestrial ecosystems over this region are considered as highly active for CO_2, water vapour, sensible and latent heat exchanges. Terrestrial ecosystems are believed to be one of the most potent sinks of atmospheric carbon dioxide (Le Quéré *et al.*, 2009,

2015). Specifically, tropical forests act as major sinks for carbon (Schimel *et al.*, 2001). India is the largest country located in SA. It is the second most populated nation in the world recording a fast economic growth over last few decades. Geographically it is bound by the Himalayas in the north, the Bay of Bengal in the east, the Arabian Sea in the west and the Indian Ocean in the south. Multiple different landscapes and ecosystems exist across India ranging from evergreen coniferous to deciduous forests. Being an agrarian country India also has a vast spread of irrigated and non-irrigated agricultural lands. However, due to the paucity of observations CO_2, water vapour and energy exchanges over these ecosystems could not be studied systematically in detail until recently when a network was proposed to be set up along the lines of Fluxnet (Sundareshwar *et al.*, 2007). Earlier, this lack of ground-based measurements compelled the researchers to use satellite-based CO_2 and LAI values for estimating GPP and NPP (Net Primary Productivity) (Chabra and Dadhwal, 2004; Nayak *et al.*, 2013). However, presence of the towering convective clouds in the tropical region makes satellite estimation of CO_2 difficult. It is often constrained by the observations from the neighbouring regions. Moreover, lack of sufficient numbers of surface measurements of CO_2 fluxes result in non-validation of satellite products (Takagi *et al.*, 2011; Valsala *et al.*, 2013). As part of NCP (National Carbon Project) by ISRO (Indian Space Research Organization) several eddy covariance (EC) flux towers were set up. Measured fluxes were used in conjunction with the MODIS surface temperature and reflectance data to calculate GPP over a wheat field in north India (Patel *et al.*, 2011). In other related studies flux and climate data were analyzed over mixed deciduous forests in central India

(Jha *et al.*, 2013), north India (Watham *et al.*, 2014) and mangrove forest in Gangetic delta in east India (Rodda *et al.*, 2016). In some cases these studies calculated the GPP using site level observations. However, none of these studies have reported GPP estimation using site level observations of LAI and its variations.

Kaziranga National Park (KNP) is a forest located in a pristine location far from the major human settlement at Tezpur in north-eastern state of Assam in India. Local climate in this region is classified as humid sub-tropical (CWa type) according to the Köppen climate classification. A 50 m tall micro-meteorological tower was erected in 2014 by IITM (Indian Institute of Tropical Meteorology Pune) in collaboration with Tezpur University as part of MetFlux India, a MoES (Ministry of Earth Sciences, Government of India) funded project in this forest (Fig. 1a) for long-term monitoring of GHG fluxes including CO_2 and water vapour. Geographical location of this tower is approximately at 26^0, $37'$ N and 93^0, $21'$ E. The tower is located at a semi-evergreen moist deciduous tall forest canopy of average height of 20 m. This tower is instrumented at multiple levels to measure weather parameters, radiation components and eddy covariance fluxes (Fig. 1b and 1c). Additional sensors have been used for soil parameters. LAI variation in this forest has not been reported so far. In the only available earlier work satellite derived NDVI (Normalized Difference Vegetation Index) data which is related to LAI were analyzed over north-east India (Saikia, 2009).

The Aggregated Canopy Model (ACM) is a simple canopy photosynthesis model which calculates daily GPP from available meteorological data sets (Williams *et al.*, 1997). It is derived from a process-based model named Soil-

Plant-Atmosphere (SPA) which acts at a much finer time scale (Williams *et al.*, 1996). GPP predicted by SPA was first validated successfully for a temperate deciduous forest against available EC data. It was then tested and calibrated globally for multiple different ecosystems, climatic conditions and driving variables (Fisher *et al.*, 2006, 2007). Main advantages of ACM are its requirement of a minimal number of input variables to run and its inherent ability to operate at fine temporal scale. Most of the process-based models require CO_2 and H_2O data at half-hourly or hourly frequency. However, continuous field measurement at such high frequency is very difficult and often not achieved. ACM can act successfully in such cases to bridge the gap between the coarse scale measurements and the GPP. In present study ACM has been used to estimate daily and annual GPP at KNP.

This paper has threefold scientific objectives. For a sub-tropical forest in India, we quantified the variations of air temperature and radiation during a one year long observation period. Second we determined the seasonal leaf phenology at the forest, and compared this to earth observations from MODIS, a satellite product. Finally, we assess the carbon sequestration potential of the forest canopy using a global calibrated ecological model.

2 Data and methods

2.1 *Data*

Air temperature was sampled every 1 min by WXT520 multi-component weather sensor manufactured by Vaisala Oyj at our observational site at

KNP at four different heights at 4 m, 7 m, 20 m and 37 m. Incoming and outgoing short-wave and long-wave radiation was measured at 20 m every 1 min by NR01 net radiometer made by Hukseflux. Additionally, half-hourly averaged records were created from both of this raw data files. The raw and averaged data files were stored in CR-3000 data-logger by Campbell Scientific. LI-7200 enclosed-path CO_2/H_2O Infra-Red Gas Analyzer (IRGA) by LI-COR was used to sample the CO_2 concentration in atmosphere at a frequency of 10 Hz at 37 m. This record was stored in a separate data-logger by LI-COR inc. Wind components were measured by a sonic anemometer Windmaster Pro by Gill Instruments, UK. The raw concentrations and wind data were subjected to rigorous quality control measures such as despiking (Vickers and Mahrt, 1997), detrending (Kaimal and Finnigan, 1994a) and co-ordinate rotations (Kaimal and Finnigan, 1994b) in EddyPro software (version 6.2.0) by LI-COR (*https* : *//www.licor.com*). EddyPro produces half-hourly averaged CO_2 mole fraction in μmol mol^{-1} (or ppm) as one of its output. This represents the amount of CO_2 present per unit amount of the moist air. The calculation assumes that the moisture has not been subtracted from the air which makes it suitable to be used as the atmospheric CO_2 concentration. LAI was measured twice a week at KNP using the hand-held LAI-2200 Leaf-Area/Plant Canopy Analyzer manufactured by LI-COR. For each LAI measurement three above-canopy and twelve below-canopy readings were taken around the tower location. Finally, single LAI value was calculated from these by internal algorithms of LAI-2200 and stored in its in-built memory. LAI value calculated this way is an average representation of the surrounding plant canopy. A detailed summary about all the variables

and measuring instruments used in the present study have been listed in Table 1.

In the present work daily average values of air temperature at 37 m, incoming solar radiation and CO_2 concentration have been calculated from their half-hourly records using R which is an open-source software ($https://www.r-project.org/$). Daily maximum and minimum values of air temperature at 37 m have also been sorted out which have further been used in the calculation of daily temperature. Few of the records had missing values which have been removed. Polynomial fits to LAI and GPP have been produced in OriginPro 8.

MODIS collection 6 data contains six scientific data layers namely FPAR, LAI, quality control (QC) and standard deviations for FPAR and LAI. Terra and Aqua combined FPAR/LAI data collection is abbreviated as MCD15A3H. It is available at a spatial resolution of 500 m and temporal resolution of 4 day. Sinusoidal grid tilling is applied to this set of data making the spatial resolution at equator to be 10^0 by 10^0. Entire data over the globe is subdivided into 648 tiles where each line of constant latitude has 36 tiles and each line of constant longitude has 18 tiles. More details about this data product can be found in the MOD15 user guide. Data is downloaded in hdf-eos (Hierarchical Data Format - Earth Observation System) format from Earthdata search client ($https://search.earthdata.nasa.gov/$). It is then further processed in MatLab. Only the data contained in the tile no. h26v06 has been used as this tile encompasses KNP. LAI values over the geographical location of 26^0, 37' N and 93^0, 21' E has been extracted from this tile along with the associated QC flag. Good quality data produced by the RT

algorithm have been retained and bad quality data using back-up algorithm or filling values have been filtered out. Satellite data retrieval often gets contaminated due to the presence of clouds especially in the tropical regions (Gao *et al.*, 2008). Hence only the data during the clear sky condition have been used.

2.2 *Model*

The Aggregated Canopy Model (ACM) has been used to calculate daily and annual GPP in our work. This model requires ten input variables to run namely Leaf Area Index (LAI in m^2 m^{-2}), average daily temperature (T_{avg} in ^{0}C), range of daily temperature (T_{range} in ^{0}C), foliar N concentration (nitro in gN m^{-2}), total daily short-wave irradiance (I in MJ m^{-2} d^{-1}), leaf-soil water potential difference (ψ_d in MPa), atmospheric CO_2 concentration (c in μmol mol^{-1} or ppm), day of year (DOY), latitude (lat in ^{0}N) and total plant-soil hydraulic resistance (R_{tot} in MPa m^2 s mili mol^{-1}). More details about these parameters including their acceptable range of variation can be found in Williams *et al.* (1997). Among all these parameters LAI, T_{avg}, T_{range}, I and c were measured at our site at KNP. Values of nitro, ψ_d and R_{tot} were prescribed as the requisite observations were not available.

2.3 *Satellite observations of LAI*

NASA's Earth Observing System (EOS) is one of the most effective platforms that produces global map of the biophysical parameters such as NDVI, FPAR (Fraction of Photosynthetically Active Radiation), LAI etc. in a regular fashion. LAI measurements are produced since June 2000 from the

surface reflectance data of Moderate Resolution Imaging Spectraradiometer (MODIS) (Myneni *et al.*, 2002). Primary LAI/FPAR algorithm of MODIS is based on a look-up-table (LUT) based procedure that exploits the spectral informations contained in MODIS red (648 nm) and near-infrared (858 nm) surface reflectances. It is also known as the RT (radiative Transfer) algorithm (Knyazikhin *et al.*, 1998). It has another backup algorithm which uses the phenomenological relationships among LAI , FPAR and NDVI in association with a global biome classification map (Yang *et al.*, 2006). MODIS LAI data set has been subjected to many extensive validation studies over multiple different ecosystems, such as croplands (Garrigues *et al.*, 2008), forest (Aragão *et al.*, 2005; Fisher and Mustard , 1997; Liang *et al.*, 2007; Tang *et al.*, 2014) etc. In these works quality controlled MODIS LAI data has been checked against in situ LAI measurements, such as LAI-2000, lidar remote sensing, digital hemispherical photography etc. to improve the applicability and interpretation of MODIS LAI data. However, despite the application of improved retrieval algorithm and filtering techniques significant mismatch exists between site measured and MODIS LAI (Biudes *et al.*, 2014). In present work an one year long time series of LAI has been extracted over KNP from MODIS Terra and Aqua combined data product. This has been plotted along with the in situ measured LAI for comparing their performances in capturing the seasonal variations in the canopy coverage.

3 Results and discussions

Very first generation of the atmospheric measurements at KNP have been used in the present work. It is first of its kind considering the fact that no such prior study exists over north-east India to date.

3.1 *Air temperature and radiation*

In this work an one year long observation period during 01^{st} July, 2015 to 30^{th} June, 2016 has been considered. Time series of multiple atmospheric variables measured during this period have been plotted in subsequent figures as explained below. Air-temperature (T) is sampled every min and a 30 min averaged record is produced from the same. Average (T_{avg}), maximum (T_{max}) and minimum (T_{min}) air-temperature have been sorted out for each day from this record. Daily range of air-temperature is defined as T_{range} = (T_{max}-T_{min})/2. T_{avg} and T_{range} for each day have been plotted in Fig. 2. Incoming and outgoing components of both Short-Wave (SW) and Long-Wave (LW) radiation are recorded at KNP every min and a 30 min averaged record is generated from the same. Daily average of Incoming SW Radiation (ISR) is calculated from this record. Total daily SW irradiance (I in MJ m^{-2} d^{-1}) is calculated from the same using the following unit conversions i.e. 1 d = (24*3600) s and 1 W = 10^{-6} MJ s^{-1}. Hence, 1 W m^{-2} = 1 J m^{-2} s^{-1} = 10^{-6} MJ m^{-2} s^{-1} = 10^{-6}*3600*24 MJ m^{-2} d^{-1}. I is plotted in Fig. 3.

T varies within 25^0-30^0C since the beginning of July to the end of September in 2015. It records a gradual decrease since the starting of October, 2015

and dips to a minimum of 12^0C during the middle of January, 2016. Gradually it starts increasing again to reach a maximum value of 30^0C at the end of June, 2016. I is seen to be more during July to September in 2015. It starts decreasing gradually since the starting of October, 2016 and dips to minimum in the middle of January, 2016. I starts increasing after that and reaches maximum again after May, 2016. Such variations in T_{avg} and I are expected and in well coherence with each other. Northern hemisphere receives more ISR during boreal summer which spans from June to September each year. As a result atmospheric air-column gets warmer. However, day to day variations in I and T during this period can be attributed to frequent occurrences of cloud and rainfall events as this is the time Indian sub-continent experiences Indian summer monsoon (ISM). Monsoon recedes after September each year. Hence, T shows a decreasing pattern during October and November in annual cycle. This period is considered as post-monsoon. During boreal winter (December to February) northern hemisphere receives less ISR and hence atmospheric air-column cools. Again, it starts receiving more ISR since March. March to May is considered as pre-monsoon period during which Indian landmass starts getting warmer due to receiving more solar insolation. This results in reversal of land-sea temperature gradient and initiates ISM. A detailed discussion of ISM is well beyond the scope of present work although.

3.2 *CO_2 concentration*

The CO_2 concentration (c) in the ambient air is measured at a frequency of 10 Hz at KNP using LI-7200. From this record daily average values of c

have been calculated and plotted in Fig. 4. Due to malfunctioning of the data-logger CO_2 values could not be stored from 20^{th} December, 2015 to 14^{th} January, 2016.

CO_2 is seen to decrease gradually from 450 μmol mol^{-1} at the beginning of July to 420 μmol mol^{-1} till the end of September, 2015. During October and November in the same year it does not monotonically increase or decrease. However, it fluctuates within a range of 420-400 μmol mol^{-1}. Farther decrease in c is recorded from 405 μmole mole^{-1} on 15^{th} January to 380 μmol mol^{-1} on 30^{th} March in 2016. It fluctuates around 380 μmol mol^{-1} in April, 2016. However, it starts increasing since the beginning of May in 2016. Till the end of June, 2016 c reaches up to 400 μmol mol^{-1}. These are above canopy c values as c is measured at a height of 37 m while average canopy height is 20 m. Hence, c bears the signature of the vegetation canopy and soil underneath. During ISM Indian landmass receives an ample amount of rainfall. Due to this water content in the soil increases. Wet soil has less CO_2 holding capacity than dry soil (Harper *et al.*, 2005). Moreover, increased microbial and decomposing activities are observed in wet soil (Sponseller, 2007). As a result of these enhanced CO_2 emission could be observed from the soil during the beginning of ISM i.e. in the starting of June. It helps in increasing the CO_2 concentration in the atmosphere. However, I and ISR are also larger during ISM compared to other times of the year. These render the soil and environment conducive for plant growth. As a result enhanced photosynthetic activity is observed during these months. It results in a gradual decrease in the atmospheric CO_2 concentration. During the dry period of winter i.e. in the months of December, January and February not much

of CO_2 emission is observed from the soil. However, during pre-monsoon period i.e. in the months on March, April and May LAI increases gradually signifying the growth of new leaves in the plants. As a result enhanced photosynthetic activity is observed bringing c further down. Moreover, soil remains dry during this period. Hence, contribution of soil emission could also remain low in atmospheric CO_2 concentration.

3.3 *Leaf Area Index (LAI)*

LAI is measured bi-weekly manually at KNP. This measurement frequency is recommended and followed by the scientific community (Walker *et al.*, 2006) as LAI does not have fast modes of variability. However, the site being located far away it is very difficult to maintain this frequency. Hence, only twenty LAI measurements could be taken instead of twenty-eight during 1^{st} July, 2015 to 10^{th} September, 2016 which are plotted in Fig. 5. To obtain annual variation of LAI a 9^{th} order polynomial was fit to this. Each calendar day of the year was assigned a serial number starting from 1 for 1^{st} January, 2015. As there are 365 days in 2015 1^{st} July, 2015 is assigned 182. On the other hand, 2016 is a leap-year having 366 days. Hence, 10^{th} September, 2016 is assigned 249. The new variable constructed this way is named 'day of year', abbreviated as DOY and used as independent variable for the polynomial fitting of LAI. This variable is also used for further analyses in this paper.

Governing equation for this fit can be written as,

$$LAI = a_1 + b_{11}.DOY + b_{12}.DOY^2 + b_{13}.DOY^3 + b_{14}.DOY^4 + b_{15}.DOY^5 + b_{16}.DOY^6 + b_{17}.DOY^7 + b_{18}.DOY^8 + b_{19}.DOY^9 \quad (1)$$

This fit has been obtained by weighted least-square method in OriginPro 8. An adjusted R-square value of 0.88 suggests the fit to be able to reproduce LAI variation with confidence during this period. This fit of LAI is also plotted in Fig. 5. More details about this fit including Standard Error (SE) for each of the fit coefficients are provided in Table 2.

For the entire period of our study LAI was enhanced during the monsoon and reduced in winter. Subsequently LAI showed increasing and decreasing patterns during pre and post-monsoon respectively. Minimum value of LAI was 0.75 in January, 2016. It reached a maximum value of 3.25 in June, 2016. Such type of LAI variation is typical of a deciduous forest (Saigusa *et al.*, 2002) where leaf shedding is observed in winter. During post-monsoon leaf senescence is observed followed by the abscission bringing the LAI down. On the other hand rapid increase in LAI is seen during pre-monsoon due to the active plant physiological growth resulting in the formation of new leaves. In situ measured LAI has a smooth pattern of variation during the period of our study. However, few deviations are observed which need to be explained. First of these occur on 29^{th} September, 2015 when LAI value is 2.5. It is more than the expected value of 2.0. Another such event is observed on 3^{rd} June, 2016. LAI recorded on this day is 3.25 which is more than the expected value of 3.0. Explaining these brings the authors a good opportunity to let the readers of this article know a bit more about the site and the difficulties

associated with it. During ISM this region receives heavy amount of rainfall. As a result the approach way to the site remains water-logged for months during and after ISM. Several feet of standing water makes the site inaccessible. However LAI measurements are conducted despite these problems. According to our observation logbook both of these days were very sunny. Moreover, as the sites were water-logged on both these days it took the observers longer than usual time to reach the measurement site via an alternate route. Due to these reasons LAI measurements could only be conducted during noon time. All other measurements were taken during morning or afternoon. These are the times of the day when diffused sunlight is present in the atmosphere and hence recommended for conducting the LAI measurement by the scientific community (Bréda, 2003; Ahl *et al.*, 2006). However, on 29^{th} November, 2015 and 3^{rd} June, 2016 this condition could not be met and measurement was carried out with the Sun being overhead. Internal algorithm of LAI-2200 for retrieving LAI suffers with difficulties in bright conditions (Aragão *et al.*, 2005; Garrigues *et al.*, 2008; Kobayashi *et al.*, 2013) which might have led to the overestimations on these two days.

3.4 *Comparison between ground-based and MODIS LAI*

Quality controlled and filtered MODIS LAI data during 1^{st} July, 2015 to 10^{th} September, 2016 has also been plotted in Fig. 5. It is evident from the figure that the MODIS LAI has a pattern of variation similar to the in situ measurements. MODIS LAI shows a decreasing trend starting from the end

of October, 2015 till the end of January, 2016. Following that an increasing trend is observed from the beginning of February till the end of May in 2016. It starts decreasing slowly from the end of June, 2016. Although this fashion of variation of MODIS LAI agrees largely with the variation of the in situ measured LAI, large variability is seen in the former. Maximum LAI recorded by the in situ measurement is 3.25 which is observed in June. However, MODIS has a significant discord with this value and its occurrence. It predicts a maximum LAI of 5.25 in October. MODIS predicts a LAI of 3.5 during June which is fairly comparable to the LAI estimate by in situ measurement around this time. In situ measurement of LAI shows minimum value to be 0.75 which occurs in January during winter. This is expected as the deciduous components of the canopy shed leaves in winter. MODIS LAI also records a similar value during this period. However, it has many abrupt and large fluctuations in winter and pre-monsoon seasons which seem to obscure the pattern of variation contained in the data. It has two unusually large deviations in the end of March and the beginning of April. These spikes report LAI value as low as 0.25. This is much smaller than the minimum value observed in winter and hence seems to be unrealistic. Although MODIS LAI follows the decreasing and increasing trends in post-monsoon and pre-monsoon absolute LAI values vary widely. Also the variation is much smoother in the ground-based in situ LAI measurement. MODIS seems to have a failure in capturing the vegetation dynamics in post-monsoon. It overestimates the LAI during this period. It overestimates the LAI during winter and pre-monsoon also. However it has lesser disagreement with in situ measured LAI in winter and pre-monsoon than in monsoon and post-

monsoon. Pre-monsoon is the time of generation of new leaves in plants. Such overestimation of LAI over forest ecosystems can occur in the MODIS product in other locations also (Aragão *et al.*, 2005; Garrigues *et al.*, 2008). Ahl *et al.* (2006) showed that MODIS products could capture the general phenology of the canopy but overestimated the LAI during the absence of leaves quite similarly to our case. In another study by (Garrigues *et al.*, 2008) LAI is shown to be overestimated by MODIS for observed LAI values more than 4. This is similar to our observation in June 2016 when LAI reported by MODIS is around 5.25 but the site-measured LAI is around 2.5. MODIS LAI is shown to have more error over Indian region by Tripathi *et al.* (2006).

This mismatch between ground-observed and MODIS LAI may result from a misrepresentation of vegetation canopy at KNP in MODIS algorithm. Since no such extensive study for validating MODIS biophysical parameters over north-east India exists before this study, it is difficult to identify the sources of error. A probable reason for the discrepancy in MODIS LAI during winter can also be the small solar zenith angle during this period (Fensholt *et al.*, 2004; Huete *et al.*, 2002).

3.5 *Modelling Gross Primary Productivity (GPP)*

Observed variables have been used as the input parameters in ACM for predicting daily GPP at KNP. Additionally, ACM requires the following variables to run. Foliar Nitrogen (N) concentration (nitro) is defined as the grams of N per square meter of leaf-area. No study has reported the nutrient contents of the plants at KNP till date. However, in an earlier work Nitrogen

contents for tropical dry deciduous and evergreen leaves were estimated to be 1.65 gN m^{-2} and 2.50 gN m^{-2} respectively (Zobel and Singh, 1997). An extensive study on distributions of leaf mass, density and thickness of woody plants spread across multiple biomes were carried out by Niinemets (1999). It suggests mean Nitrogen content to be 1.79 gN m^{-2} with a standard deviation (SD) of 0.98 gN m^{-2}. In our work nitro has been set at 1.9 gN m^{-2}. Hence total foliar N concentration became 1.9*LAI gN m^{-2}.

Leaf-soil water potential difference (ψ_d) is defined as the difference between canopy minimum leaf water potential and soil water potential (Williams *et al.*, 1997). The more negative this parameter is, the more is the available water to the canopy. As described earlier in the introduction KNP is located in north-east India. Annually this region receives heavy amount of rainfall ($\sim$ 2346 mm) (Jain *et al.*, 2013). Forest floor inundation is also observed at several places. Hence, no water stress was assumed to be present and ψ_d was set at -2.5 MPa. Total plant-soil hydraulic resistance (R_{tot}) is a coarse-scale agglomeration of fine-scale SPA model drivers. It is a combination of soil hydraulic resistance, root, leaf and stem dimensions (Williams *et al.*, 1996). The more is the canopy height, the more is the R_{tot}. However, relative control of R_{tot} on GPP is much less than other driving variables. Moreover, in well-watered or no drought-stress condition it becomes even less significant (Williams *et al.*, 1997). In present work R_{tot} has been set at 1.0 MPa m^2 s $mmol^{-1}$. Calculated daily GPP have been plotted in Fig. 6. There exists a gap of almost three weeks in observed GPP due to missing CO_2 values as explained earlier. Hence to estimate annual variation of GPP a 9^{th} order polynomial was fit to the observed values which can be expressed

mathematically as,

$$GPP = a_2 + b_{21}.DOY + b_{22}.DOY^2 + b_{23}.DOY^3 + b_{24}.DOY^4 + b_{25}.DOY^5 + b_{26}.DOY^6 + b_{27}.DOY^7 + b_{28}.DOY^8 + b_{29}.DOY^9 \quad (2)$$

Weighted least-square method was used in OriginPro 8 for above this curve-fitting. Adjusted R-square value for this fit is 0.74 suggesting the fit to be a good representation of annual GPP variation. This fit of GPP is plotted in Fig. 7. Details about this fit including Standard Error (SE) for each of the fit coefficients can be found in Table 3.

Fit of daily GPP was integrated to calculate annual GPP (Fig. 7). Period of the integration was kept as one year from 1^{st} July, 2015 to 30^{th} June, 2016. It was same as the period of the observation, as described earlier. Calculated this way, annual GPP turns out to be approximately equal to 2110 gC m^{-2} $year^{-1}$ or 2.11 kgC m^{-2} $year^{-1}$.

Daily GPP shows a well-defined pattern of annual variation. Maximum daily GPP is observed during monsoon. It decreases gradually during post-monsoon to a minimum in winter. It starts increasing in pre-monsoon before reaching maximum again in monsoon. From the polynomial fit maximum daily GPP is seen to be 11.5 gC m^{-2} d^{-1} in June, 2016. It is minimum at 1.5 gC m^{-2} d^{-1} in December, 2015. Integrated GPP during July to September, 2015 is 750 gC m^{-2}. At the end of February and June, 2016 integrated daily GPP are 1100 gC m^{-2} and 2100 gC m^{-2} respectively. Hence integration of daily GPP shows that cumulative daily GPP records rapid increments during monsoon and pre-monsoon and slower growths during post-monsoon and winter. In other words probability of carbon sequestration is maximum

during monsoon and pre-monsoon. Such a seasonal variation in plant productivity has been reported by (Nayak *et al.*, 2010). In this work authors have modelled Net Primary Productivity (NPP) over different ecosystems in India using satellite derived input data and a terrestrial biosphere model. This study shows that the onset of ISM by the end of June triggers an increase in NPP. According to this study broadleaf deciduous and evergreen forests record second and third largest NPP over Indian landmass after croplands. However, it can not be directly compared with our estimates due to two reasons. Firstly, NPP is a net estimate whereas GPP is a gross one. Auto and heterotrophic respiration components need to be subtracted from GPP for calculating NPP. However, in present work respiration components are not calculated. Secondly, in present work in situ measurements of weather variables and LAI have been used for modelling GPP. Researchers have used satellite derived weather parameters and LAI also for modelling GPP and NPP (Barman *et al.*, 2014; Verma *et al.*, 2014). Satellite-based GPP and NPP products are also available as MOD17 product (Turner *et al.*, 2003; Wang *et al.*, 2013). However, either of these estimates tend to have bias compared to ground-based estimates and hence are less reliable as reported by many researchers (Heinsch *et al.*, 2006; Liu *et al.*, 2014; Neumann *et al.*, 2006).

Annual GPP for multiple deciduous forests located in different climatic regions have been reported by many researchers (Goulden *et al.*, 1996; Barford *et al.*, 2001). For a cool temperate deciduous forest in Japan it was estimated to be 1.146 kgC m^{-2} $year^{-1}$ (Saigusa *et al.*, 2002). Annual GPP for a temperate deciduous hardwood forest in north-eastern United States

was calculated to be 1.639 kgC m^{-2} $year^{-1}$ (Turner *et al.*, 2003). For a tropical semi-deciduous forest in Amazon basin El-Masri *et al.* (2013) simulated the same to be 2.66 kgC m^{-2} $year^{-1}$. However, due to unavailability of data very few of such studies exist for Indian forests. In one of such studies GPP was estimated to be 1.271 kgC m^{-2} $year^{-1}$ for a mangrove forest (Rodda *et al.*, 2016) in Gangetic delta over Bay of Bengal. In our study annual GPP is estimated to be 2.11 kgC m^{-2} $year^{-1}$. This is similar to the predicted values by global modelling studies done by Barman *et al.* (2014). A global scale simulation for upscaling carbon and water fluxes done by Jung *et al.* (2011) using a machine learning technique Fluxnet-MTE (Model tree Ensemble) also predicts the similar value of GPP over KNP. Positive and negative values of GPP represent sinking and sourcing of carbon respectively. Hence our result indicates at the possibility of a large amount of carbon sequestration at annual scale at KNP. However, actual carbon sequestration will be less than GPP and can only be inferred from NPP which is an absolute measure of net carbon exchange between the atmosphere and the biosphere.

4 Summary

In present work one year long observational records of LAI, air temperature, incoming short-wave radiation and atmospheric CO_2 concentration measured by a micrometeorological flux tower over the forest ecosystem at Kaziranga National Park during July 2015 to June 2016 have been presented. These variables have also been used as inputs in Aggregated Canopy Model for es-

timating the annual GPP of this forest ecosystem. This forest is identified as a semi-evergreen moist deciduous forest located in a humid sub-tropical environment. This is the very first time that the annual variation of LAI has been studied for a tropical forest ecosystem located in north-east India. The LAI is seen to vary between 0.75 in winter to 3.25 in summer. The ground-based in situ measured LAI is seen to capture the vegetation phenology in a more efficient way than MODIS. Annual GPP at Kaziranga National Park is estimated to be 2.11 kgC m^{-2} $year^{-1}$. This is also the very first time that carbon sequestration potential of any forest in north-east India has been studied. In this work GPP has been calculated using daily scale meteorological variables. No fine scale variable such as high-frequency flux has been used in this calculation.

Present work provides with the first ever ground-based LAI and GPP estimates from this part of the globe. This is expected to fill the gaps in data availability as well as scientific understanding of the vegetation dynamics from this region. Specifically, this data set will be immensely beneficial for the modelling community. The GPP estimate calculated in this work needs to be validated against the GPP calculated by upscaling the ground-based fluxes. Authors of the present paper plan to continue this study with further calculations of high frequency eddy covariance fluxes of CO_2, water and energy. More micrometeorological flux towers are being established over different unique and pristine ecosystems in India under the aegis of the MetFlux India project. This is expected to generate a continuous long-term database of good quality climate and flux data over India in near future.

Acknowledgements

Our sincere gratitude to the Director, IITM for all his constant encouragement and support. We thank all the members of the project team for all possible help. CCCR (Centre for Climate Change Research) is part of Indian Institute of Tropical Meteorology, Pune (IITM) and is fully supported by the Earth System Science Organization (ESSO) of Ministry of Earth Sciences (MoES), Government of India. A special thanks to Dr. Stephan Matthiesen, GAUGE (Greenhouse gAs Uk and Global Emissions) UK for conducting International Summer School on Global greenhouse Gases in 2016.

References

Ahl D E, Gower Stith T., Burrows S N, Shavanov N V, Myneni R B , Knyazikhin Y 2006 Monitoring spring canopy phenology of a deciduous broadleaf forest using MODIS; *Remote Sens. Environ.* **104** 88–95.

Aragão L E O C, Shimabukuro Y E, Espirito-Santo F D B and Williams M 2005 Spatial validation of the collection 4 MODIS LAI product in Eastern Amazonia; *IEEE Trans. Geosci. Remote Sens.* **43** 2526–2534.

Baldocchi D, Falge E, Gu L, Olson R et al. 2001 FLUXNET: A new tool to study the temporal and spatial variability of ecosystem-scale carbon dioxide, water vapor, and energy flux densities; *Bull. Am. Meteor. Soc.* **82** 2415–2434.

Barford C C, Wofsy S C, Goulden M L, Munger J W, Pyle E H, Urbanski S P, Hutyra L, Saleska S R, Fitzjarrald D and Moore K 2001 Factors

Controlling Long-and Short-Term Sequestration of atmospheric CO_2 in a Mid-latitude Forest; *Science* **294** 1688–1691.

Barman R, Jain A K and Liang M 2014 Climate-driven uncertainties in modeling terrestrial gross primary production: a site level to global-scale analysis; *Global Change Biol.* **20** 1394–1411.

Beringer J, Hutley L B, McHugh I, Arndt S K, Campbell,D, Cleugh,H A, Cleverly,J, Resco de Dios,V, Eamus D, Evans B et al. 2016 An introduction to the Australian and New Zealand flux tower network–Ozflux; *Biogeosci.* **13** 5895–5916.

Biudes M S, Machado N G, Danelichen V H D M, Souza M C, Vourlitis G L and Nogueira J D S, 2014 Ground and remote sensing-based measurements of leaf area index in a transitional forest and seasonal flooded forest in Brazil; *Int. J. Biometeorol.* **58** 1181–1193.

Boden T A, Krassovski M and Yang B 2013 The AmeriFlux data activity and data system: an evolving collection of data management techniques, tools, products and services; *Geosci. Instrum. Methods Data Sys.* **2** 165–176.

Bonan G B (1995). Land-atmosphere CO_2 exchange simulated by a land surface process model coupled to an atmospheric general; *J. Geophys. Res.* **100** 2817–2831.

Bonan G B, Lawrence P J, Oleson K W, Levis S, Jung M, Reichstein M, Lawrence D M and Swenson S C 2011 Improving canopy processes in the Community Land Model version 4 (CLM4) using global flux fields

empirically inferred from FLUXNET data; *J. Geophys. Res.: Biogeosci.* **116(G02014)**, doi: 10.1029/2010JG001593.

Bréda, N J 2003 Ground-based measurements of leaf area index: a review of methods, instruments and current controversies; *J. Exp. Bot.* **54** 2403–2417.

Chabra A and Dadhwal V K 2004 Estimating terrestrial net primary productivity over India using satellite data; *Curr. Sci.* **86** 269–271.

Chapin III F S, Woodwell G M, Randerson J T, Rastetter E B, Lovett G M, Baldocchi D D, Clark D A, Harmon M E, Schimel D S, Valentini R et al. 2006 Reconciling carbon-cycle concepts, terminology, and methods; *Ecosystems* **9** 1041–1050.

Chen J M, Govind A, Sonnentag O, Zhang Y, Barr A and Amiro B 2006 Leaf area index measurements at Fluxnet Canada forest sites; *Agric. For. Meteorol.* **140** 257–268.

Coops N C, Black, T A, Jassal R P S, Trofymow J T and Morgenstern K 2007 Comparison of MODIS, eddy covariance determined and physiologically modelled gross primary production (GPP) in a Douglas-fir forest stand; *Remote Sens. Environ.* **107** 385–401.

Curtis P S, Hanson P J, Bolstad P, Barford C, Randolph J, Schmid H and Wilson K B 2002 Biometric and eddy-covariance based estimates of annual carbon storage in five eastern North American deciduous forests *Agric. For. Meteorol.* **113** 3–19.

El-Masri B, Barman R, Meiyappan P, Song Y, Liang M and Jain A K 2013 Carbon dynamics in the Amazonian basin: Integration of eddy covariance and ecophysiological data with a land surface model; *Agric. For. Meteorol.* **182** 156–167.

Fensholt R, Sandholt I, Rasmussen M S, 2004 Evaluation of MODIS LAI, fAPAR and the relation between fAPAR and NDVI in a semi-arid environment using in situ measurements. *Remote Sens. Environ.* **91** 490–507.

Fisher J I and Mustard J F 2007 Cross-scalar satellite phenology from ground, Landsat, and MODIS data; *Remote Sens. Environ.* **109** 261–273.

Fisher R A, Williams M, Do V, Lobo R, Costa A L D and Meir P 2006 Evidence from Amazonian forests is consistent with isohydric control of leaf water potential; *Plant Cell Environ.* **29** 151–165.

Fisher R, Williams M, Costa D, Lola A, Malhi Y, Costa R D, Almeida S and Meir P 2007 The response of an Eastern Amazonian rain forest to drought stress: results and modelling analyses from a throughfall exclusion experiment; *Global Change Biol.* **13** 2361–2378.

Gao F, Morisette J, Wolfe R E, Ederer G, Pedelty J, Masuoka E, Myneni R, Tan B and Nightingale J 2008 An algorithm to produce temporally and spatially continuous MODIS-LAI time series; *IEEE Geosci. Remote Sens. Lett.* **5** 60–64.

Garbulsky M F, Peñuelas J, Papale D, Ardö J, Goulden M L, Kiely G, Richardson A D, Rotenberg E, Veenendaal E M and Filella I 2010 Patterns and controls of the variability of radiation use efficiency and primary

productivity across terrestrial ecosystems; *Global Ecol. Biogeogr.* **19** 253–267.

Garrigues S, Shabanov N V, Swanson K, Morisette J, Baret F and Myneni R B, 2008 Intercomparison and sensitivity analysis of Leaf Area Index retrievals from LAI-2000, AccuPAR, and digital hemispherical photography over croplands; *Agric. For. Meteorol.* **148** 1193–1209.

Garrigues S, Lacaze R, Baret F J T M, Morisette J T, Weiss M, Nickeson J E, Fernandes R, Plummer S, Shavanov N V, Myneni R B et al. 2008 Validation and intercomparison of global Leaf Area Index products derived from remote sensing data; *J. Geophys. Research:. Biogeosci.* **113(G02028)** doi: 10.1029/2007JG000635.

Gitelson A A, Peng Y, Masek J G, Rundquist D C, Verma S, Suyker A, Baker J M, Hatfield J L and Meyers T 2012 Remote estimation of crop gross primary production with Landsat data; *Remote Sens. Environ.* **121** 404–414.

Goulden M L, Munger J W, Fan S-M, Daube B C and Wofsy S C 1996 Exchange of carbon dioxide by a deciduous forest: response to interannual climate variability; *Science* **271** 1576–1578.

Gower S T, Kucharik C J and Norman J M 1999 Direct and Indirect Estimation of Leaf Area Index, f_{APAR}, and Net Primary Production of Terrestrial Ecosystems; *Remote Sens. Environ.*, **70** 29–51.

Grace J, Malhi Y, Lloyd J, McIntyre J, Miranda A C, Meir P and Miranda

H S 1996 The use of eddy covariance to infer the net carbon dioxide uptake of Brazilian rain forest; *Global Change Biol.*, **2** 209–217.

Harper C W, Blair J M, Fay P A, Knapp A K and Carlisle J D 2005 Increased rainfall variability and reduced rainfall amount decreases soil CO_2 flux in a grassland ecosystem; *Global Change Biol.*, **11** 322–334.

Heinsch F A, Zhao M, Running S W, Kimball J S, Nemani R, Davis K J, Bolstad P V, Cook B D, Desai A R, Ricciuto, D M et al. 2006 Evaluation of remote sensing based terrestrial productivity from MODIS using regional tower eddy flux network observations; *IEEE Trans. Geosci. Remote Sens.* **7** 1908–1925.

Huete A, Didan K, Miura T, Rodriguez E P, Gao X and Ferreira L G, 2002 Overview of the radiometric and biophysical performance of the MODIS vegetation indices; *Remote Sens. Environ.* **83** 195–213.

Jain S, Kumar V and Saharia M 2013 Analysis of rainfall and temperature trends in northeast India; *Int. J. Climatol.* **33** 968–978.

Jha C S, Thumaty K C, Rodda S R, Sonakia A and Dadhwal V K 2013 Analysis of carbon dioxide, water vapour and energy fluxes over an Indian teak mixed deciduous forest for winter and summer months using eddy covariance technique; *J. Earth Syst. Sci.* **122** 1259–1268.

Jonckheere I, Fleck S, Nackaerts K, Muys B, Coppin P, Weiss M and Baret F 2004 Review of methods for in situ leaf area index determination: Part I. theories, sensors and hemispherical photography; *Agric. For. Meteorol.* **121** 19–35.

Jung M, Reichstein M, Margolis H A, Cescatti A, Richardson A D, Arain M A, Arneth A, Bernhofer C, Bonal D, Chen J et al. 2011 Global patterns of land-atmosphere fluxes of carbon dioxide, latent heat, and sensible heat derived from eddy covariance, satellite, and meteorological observations; *J. Geophys. Res.: Biogeosci.* **116(G00J07)** dor: 10.1029/2010JG001566.

Kaimal J C and Finnigan J J 1994 *Atmospheric Boundary Layer Flows: Their Structure and Measurement*; United States of America Oxford University Press 264–266

Kaimal J C and Finnigan J J 1994 *Atmospheric Boundary Layer Flows: Their Structure and Measurement*; United States of America Oxford University Press 234–240

Knyazikhin Y, Martonchik J V, Myneni R B, Diner D J and Running S W, 1998 Synergistic algorithm for estimating vegetation canopy leaf area index and fraction of absorbed photosynthetically active radiation from MODIS and MISR data; *J. Geophys.l Res.* **103** 32257–32276.

Kobayashi H, Ryu Y, Baldocchi D D, Welles J M and Norman J M . 2013 On the correct estimation of gap fraction: How to remove scattered radiation in gap fraction measurements?; *Agric. For. Meteorol.* **174** 170–183.

Le Quéré C, Raupach M R, Canadell J G, Marland G, Bopp L, Ciais P, Conway T J, Doney S C, Feely R A, Foster P et al. 2009 Trends in the sources and sinks of carbon dioxide; *Nat. Geosci.* **2** 831–836.

Le Quéré C, Moriarty R, Andrew R M, Peters G P, Ciais G P, Friedlingstein

P, Jones S D, Sitch S, Tans P, Arneth A et al. 2015 Global carbon budget 2014. *Earth Syst. Sci. Data*; **7** 47–85.

Liang L, Schwartz M D and Fei S 2011 Validating satellite phenology through ground observation and landscape scaling in a mixed seasonal forest; *Remote Sens. Environ.* **115** 143157.

Liu Z, Shao Q and Liu J 2014 The performances of MODIS-GPP and-ET products in China and their sensitivity to input data (FPAR/LAI); *Remote Sens.* **7** 135–152.

Mizoguchi Y, Miyata A, Ohtani Y, Hirata R and Yuta S 2009 A review of tower flux observation sites in Asia; *J. For. Res.* **14** 1–9.

Muraoka H, Saigusa N, Nasahara K N, Noda H, Yoshino J, Saitoh T M, Nagai S, Murayama S and Koizumi H 2010 Effects of seasonal and interannual variations in leaf photosynthesis and canopy leaf area index on gross primary production of a cool-temperate deciduous broadleaf forest in Takayama, Japan; *J. Plant Res.*, **123**,; 563–576.

Myneni R B, Hoffman S, Knyazikhin Y, Privette J L, Glassy J, Tian Y, Wang Y, Song S, Zhang Y, Smith G R et al. 2002 Global products of vegetation leaf area and fraction absorbed PAR from year one of MODIS data; *Remote Sens. Environ.* **83** 214–231.

Nayak R K, Patel N R and Dadhwal V K . 2010 Estimation and analysis of terrestrial net primary productivity over India by remote-sensing-driven terrestrial biosphere model; *Environ. Monit. Assess.* **170** 195–213.

Nayak R, Patel N and Dadhwal V K 2013. Inter-annual variability and climate control of terrestrial net primary productivity over India; *Int. J. Climatol.*, **33** 132–142.

Neumann M, Zhao M, Kinderman G. and Hasenauer H. 2015 Comparing MODIS net primary production estimates with terrestrial national forest inventory data in Austria; *Remote Sens.* **7** 3878–3906.

Niinemets, Ü 1999 Research review. components of leaf dry mass per area–thickness and density–alter leaf photosynthetic capacity in reverse directions in woody plants; *New Phytol.*, **144** 35–47.

Patel N, Dadhwal V and Saha S 2011 Measurement and scaling of carbon dioxide (CO_2) exchanges in wheat using flux-tower and remote sensing; *J. Indian Soc. Remote Sens.* **39** 383–391.

Rodda S R, Thumaty K C, Jha C S and Dadhwal V K 2016 Seasonal variations of carbon dioxide, water vapor and energy fluxes in tropical Indian mangroves; *Forests* **7** 35.

Saigusa N, Yamamoto S, Murayama S and Kondo H 2005 Inter-annual variability of carbon budget components in an AsiaFlux forest site estimated by long-term flux measurements; *Agric. For. Meteorol.* **134** 4–16.

Saigusa N, Yamamoto S, Murayama S, Kondo H and Nishimura N 2002 Gross primary production and net ecosystem exchange of a cool-temperate deciduous forest estimated by the eddy covariance method; *Agric. For. Meteorol.* **112** 203–215.

Saikia A 2009 NDVI variability in North East India; *Scott. Geogr. J.* **125** 195–213.

Schaefer K, Schwalm C R, Williams C, Arain M A, Barr A, Chen J M, Davis K J, Dimitrov D, Hilton T W, Hollinger D Y et al. 2012 A model-data comparison of gross primary productivity: Results from the North American Carbon Program site synthesis; *J. Geophys. Res.: Biogeosci.* **117(G03010)** doi: 10.1029/2012JG001960.

Schimel D S, House J I, Hibbard K A, Bousquet P, Ciais P, Peylin P, Braswell B H, Apps M J, Baker D, Bondeau A et al. 2001 Recent patterns and mechanisms of carbon exchange by terrestrial ecosystems; *Nature* **414** 169–172.

Sellers P, Dickinson R, Randall D, Betts A, Hall F, Berry J, Collatz G, Denning A, Mooney H, Nobre C et al. 1997 Modeling the exchanges of energy, water, and carbon between continents and the atmosphere; *Science* **275** 502–509.

Solberg S, Brunner A, Hanssen K H, Lange H, Næsset E, Rautiainen M and Stenberg P 2009 Mapping LAI in a Norway spruce forest using airborne laser scanning; *Remote Sens. Environ.* **113** 2317–2327.

Sponseller R A 2007 Precipitation pulses and soil CO_2 flux in a Sonoran desert ecosystem; *Global Change Biol.* **13** 426–436.

Sundareshwar P, Murtugudde R, Srinivasan G, Singh S, Ramesh K, Ramesh R, Verma S, Agarwal D, Baldocchi D, Baru C et al. 2007 Environmental monitoring network for India; *Science* **316** 204–205.

Takagi H, Saeki T, Oda T, Saito M, ValsalaV, Belikov D, Saito R, Yoshida Y, Morino I, Uchino O et al. 2011 On the benefit of GOSAT observations to the estimation of regional CO_2 fluxes; *Sola* **7** 161–164.

Tang H, Brolly M, Zhao F, Strahler A H, Schaaf C L, Ganguly S, Zhang G and Dubayah R, 2014 Deriving and validating Leaf Area Index (LAI) at multiple spatial scales through lidar remote sensing: A case study in Sierra National Forest, CA; *Remote Sens. Environ.* **143** 131–141.

Tripathi R, Sahoo R N, Gupta V K, Sehgal V K and Sahoo P M 2013 Retrieval of Leaf Area Index using IRS-P6, LISS-III data and validation of MODIS LAI product (MOD15 V5) over trans Gangetic Plains of India; *Indian J. Agr. Sci* **83** 380–385.

Turner D P, Ritts W D, Cohen W B, Gower S T, Zhao M, Running S W, Wofsy S C, Urbanski S, Dunn A L and Munger J 2003 Scaling gross primary production (GPP) over boreal and deciduous forest landscapes in support of MODIS GPP product validation; *Remote Sens. Environ.* **88** 256–270.

Valsala V, Tiwari Y K, Pillai P, Roxy M, Maksyutov S and Murtugudde R 2013 Intraseasonal variability of terrestrial biospheric CO_2 fluxes over india during summer monsoons; *J. Geophys. Res.: Biogeosci.* **118** 752–769.

Verma M, Friedl M A, Richardson A D, Kiely G, Law B E, Cescatti A, Wohlfart G, Gielen B, Roupsard O, Moors, E J et al. 2014 Remote sensing of annual terrestrial gross primary productivity from MODIS: an assessment using the FLUXNET La Thuile data set; *Biogeosci.* **11** 2185–2200.

Vickers D and Mahrt L 1997 Quality control and flux sampling problems for tower and aircraft data; *J. Atmos. Ocean. Tech.* **14** 512–526.

Walker J, Robarge W, Wu Y and Meyers T 2006 Measurement of bi-directional ammonia fluxes over soybean using the modified Bowen-ratio technique; *Agric. For. Meteorol.* **138** 54–68.

Wang X, Ma M, Li X, Song Y, Tan J, Huang G, Zhang Z, Zhao T, Feng J, Ma Z et al. 2013 Validation of MODIS-GPP product at 10 flux sites in northern China; *Int. J. Remote Sens.* 34 587–599.

Watham T, Kushwaha S, Patel N and Dadhwal V 2014 Monitoring of carbon dioxide and water vapour exchange over a young mixed forest plantation using eddy covariance technique; *Curr. Sci.* **107** 857–867.

Watson D J 1947 Comparative Physiological Studies on the Growth of Field Crops: I. Variation in Net Assimilation Rate and Leaf Area between Species and Varieties, and within and between Years; *Ann. Bot.* **11** 41–76.

Williams M, Rastetter E, Fernandes D, Goulden M, Wofsy S, Shaver G, Melillo J, Munger J, Fan S M and Nadelhoffer K 1996 Modelling the soil-plant-atmosphere continuum in a Quercus–Acer stand at Harvard Forest: the regulation of stomatal conductance by light, nitrogen and soil/plant hydraulic properties; *Plant Cell Environ.* **19** 911–927.

Williams M, Rastetter E B, Fernandes D N, Goulden M L, Shaver G R and Johnson L C 1997 Predicting gross primary productivity in terrestrial ecosystems; *Ecol.Appl.* **7** 882–894.

Wu C, Chen J M and Huang N 2011) Predicting gross primary production from the enhanced vegetation index and photosynthetically active radiation: Evaluation and calibration; *Remote Sens. Environ.* **115** 3424–3435.

Yang W, Tan B, Huang D, Rautiainen M, Shabanov N V, Wang Y, Privette J L, Huemmrich K F, Fensholt R, Sandholt Iet al, 2006 MODIS Leaf Area Index Products: From Validation to Algorithm Improvement; *IEEE Trans. Geosci. Remote Sens.* **44** 1885–1898.

Zobel D B and Singh S P 1997 Himalayan forests and ecological generalizations; *BioScience* **47** 735–745.

5 Figure Captions

1. (a) 50 m tall micrometeorological tower at KNP; (b) deciduous forest canopy at KNP as seen from the tower; (c) multi-component weather sensor and net radiometer over the vegetation canopy as seen from the tower.

2. Observed daily mean and range of air temperature (in Red and Violet respectively) during 01^{st} July, 2015 to 30^{th} June, 2016.

3. Observed daily averaged incoming short-wave radiation during 01^{st} July, 2015 to 30^{th} June, 2016.

4. Observed daily averaged CO_2 mole fraction during 01^{st} July, 2015 to 30^{th} June, 2016.

5. Measured, MODIS-derived and fit LAI during 01^{st} July, 2015 to 10^{th} September, 2016.

6. Modelled daily GPP using ACM during 01^{st} July, 2015 to 30^{th} June, 2016.

7. Polynomial fit to the modelled daily GPP and annual GPP calculated by

integrating the fit during 01^{st} July, 2015 to 30^{th} June, 2016.

Table 1: *Variables used in present study*

variable	abbreviation	unit	measuring instrument/sensor, manufacturer	measurement height (m)
air-temperature	T	^{0}C	WXT520 multi-component weather transmitter, Vaisala	37
incoming short-wave (SW) radiation	ISR	W m^{-2}	NR-01 4-component net radiometer, Hukseflux	20
CO_2 concentration	c	μmol mol^{-1}	LI-7200 enclosed path CO_2/H_2O analyzer, Licor inc.	37
Leaf-Area Index	LAI	m^2 m^{-2}	LAI-2200 Leaf-Area/Plant Canopy Analyzer, Licor inc.	ground level

Table 2: *Polynomial fit coefficients for LAI*

fit coefficients of LAI	value	Standard Error (SE)
a_1	0	0
b_{11}	$2.85*10^{-14}$	$3.29*10^{-15}$
b_{12}	$3.85*10^{-12}$	$4.44*10^{-13}$
b_{13}	$4.10*10^{-10}$	$4.74*10^{-11}$
b_{14}	$2.64*10^{-8}$	$3.04*10^{-9}$
b_{15}	$-2.73*10^{-10}$	$3.56*10^{-11}$
b_{16}	$1.11*10^{-12}$	$1.63*10^{-13}$
b_{17}	$-2.23*10^{-15}$	$3.65*10^{-16}$
b_{18}	$2.21*10^{-18}$	$4.02*10^{-19}$
b_{19}	$-8.62*10^{-22}$	$1.74*10^{-22}$

Table 3: *Polynomial fit coefficients for GPP*

fit coefficients of GPP	value	Standard Error (SE)
a_2	0	0
b_{21}	$1.33*10^{-13}$	$1.06*10^{-14}$
b_{22}	$1.68*10^{-11}$	$1.34*10^{-12}$
b_{23}	$1.66*10^{-9}$	$1.31*10^{-10}$
b_{24}	$9.75*10^{-8}$	$7.73*10^{-9}$
b_{25}	$-1.07*10^{-9}$	$1.04*10^{-10}$
b_{26}	$4.69*10^{-12}$	$5.44*10^{-13}$
b_{27}	$-1.09*10^{-14}$	$1.40*10^{-15}$
b_{28}	$1.11*10^{-17}$	$1.76*10^{-18}$
b_{29}	$-4.77*10^{-21}$	$8.73*10^{-22}$

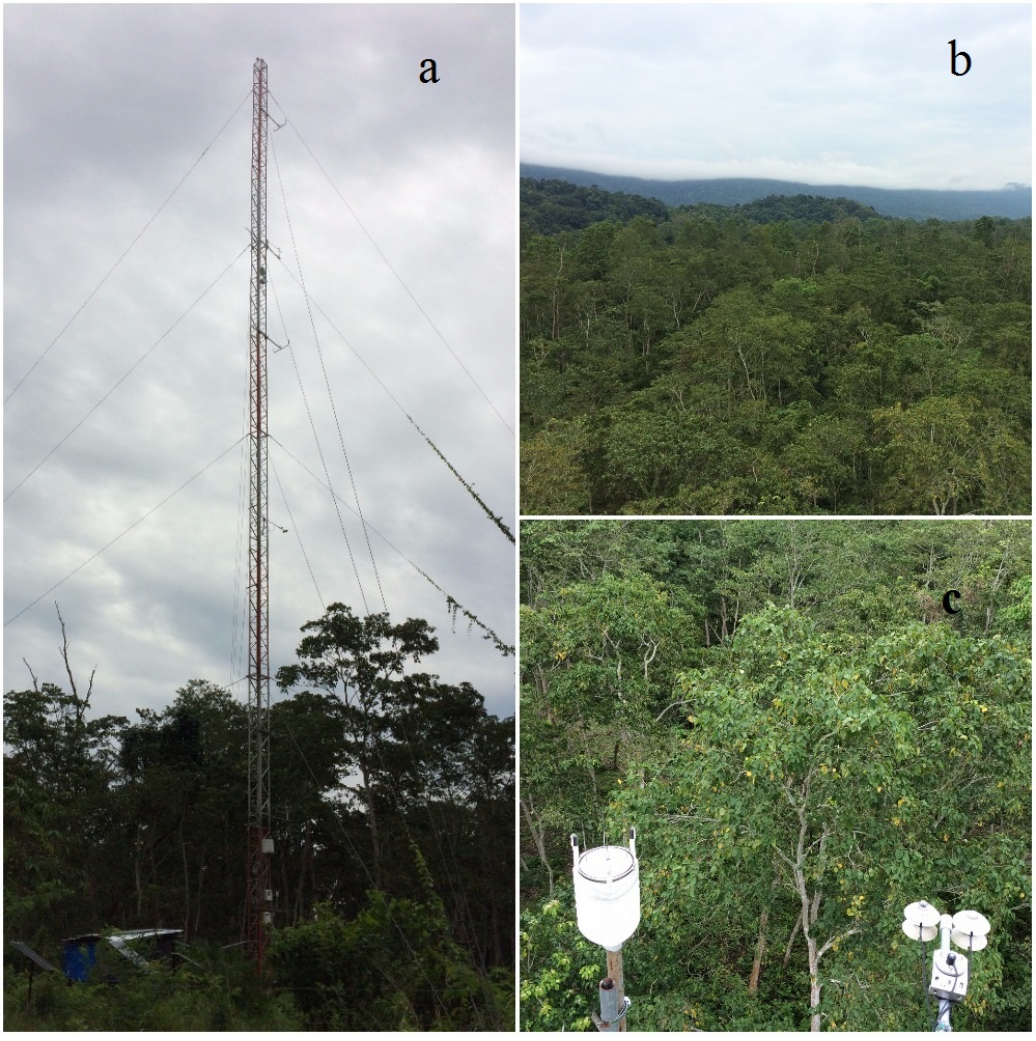

Figure 1: 1. (a) 50 m tall micrometeorological tower at KNP; (b) deciduous forest canopy at KNP as seen from the tower; (c) multi-component weather sensor and net radiometer over the vegetation canopy as seen from the tower.

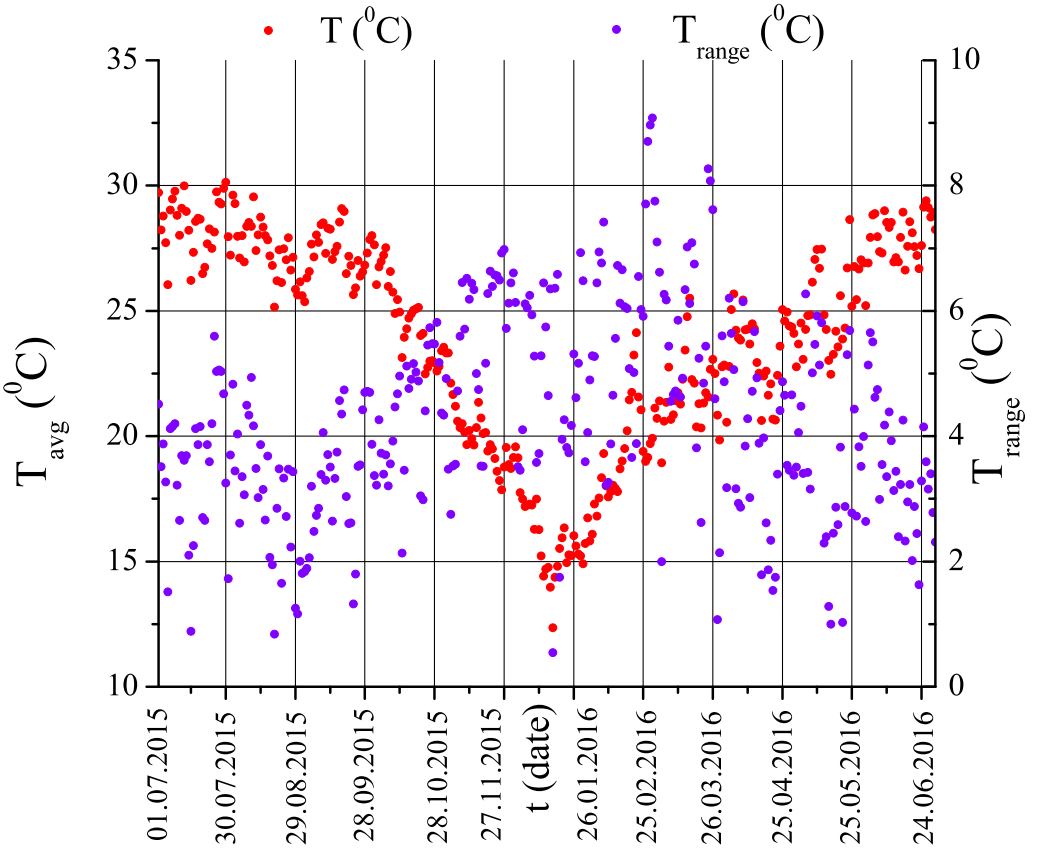

Figure 2: Observed daily mean and range of air temperature (in Red and Violet respectively) during 01^{st} July, 2015 to 30^{th} June, 2016.

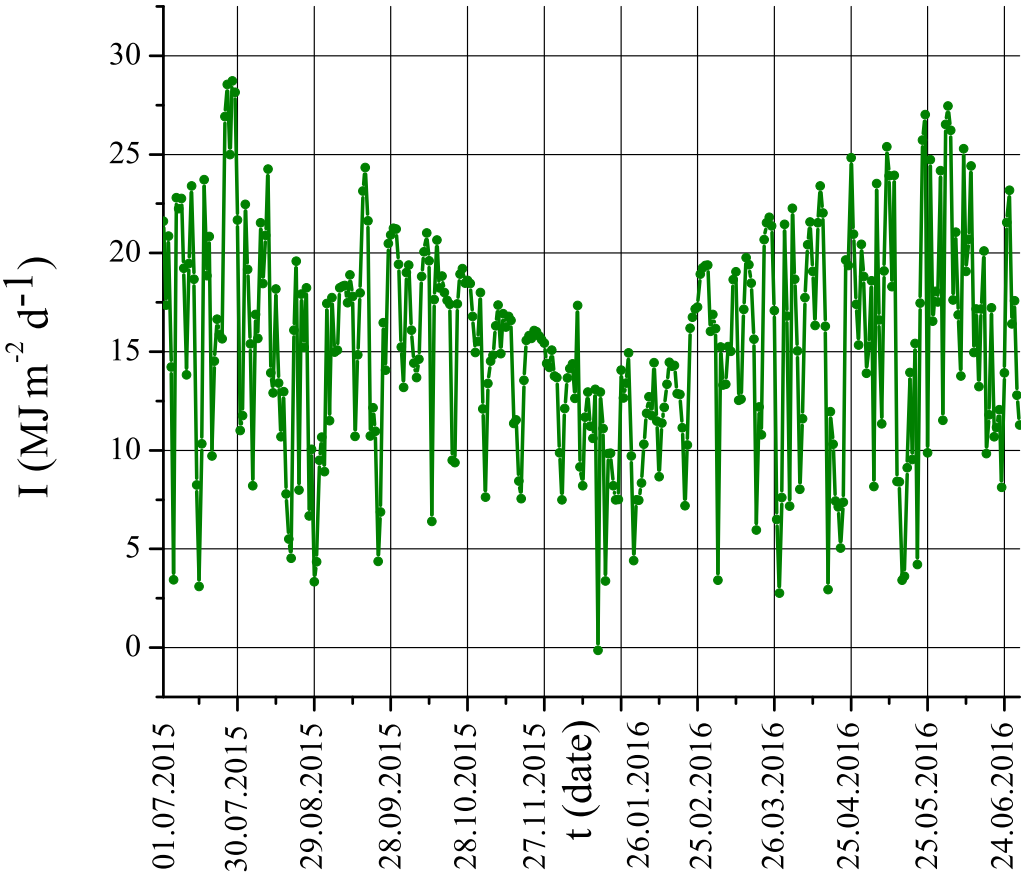

Figure 3: Observed daily averaged incoming short-wave radiation during 01^{st} July, 2015 to 30^{th} June, 2016.

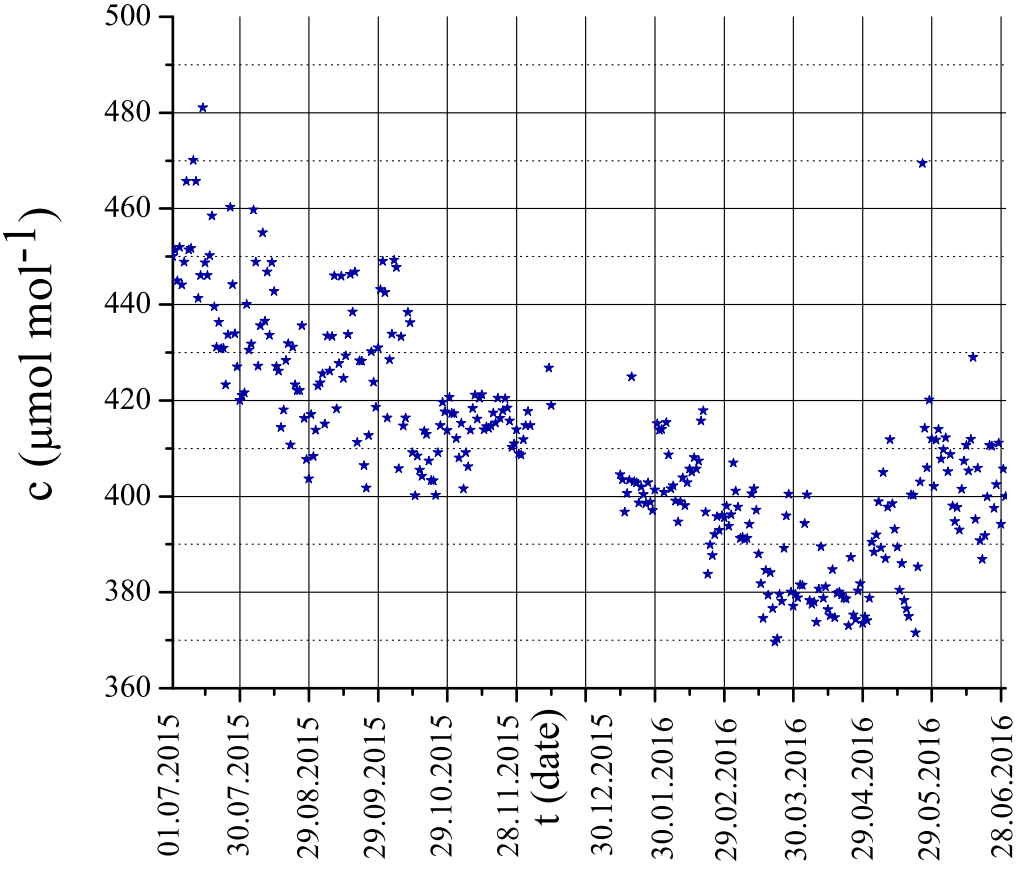

Figure 4: Observed daily averaged CO_2 mole fraction during 01^{st} July, 2015 to 30^{th} June, 2016.

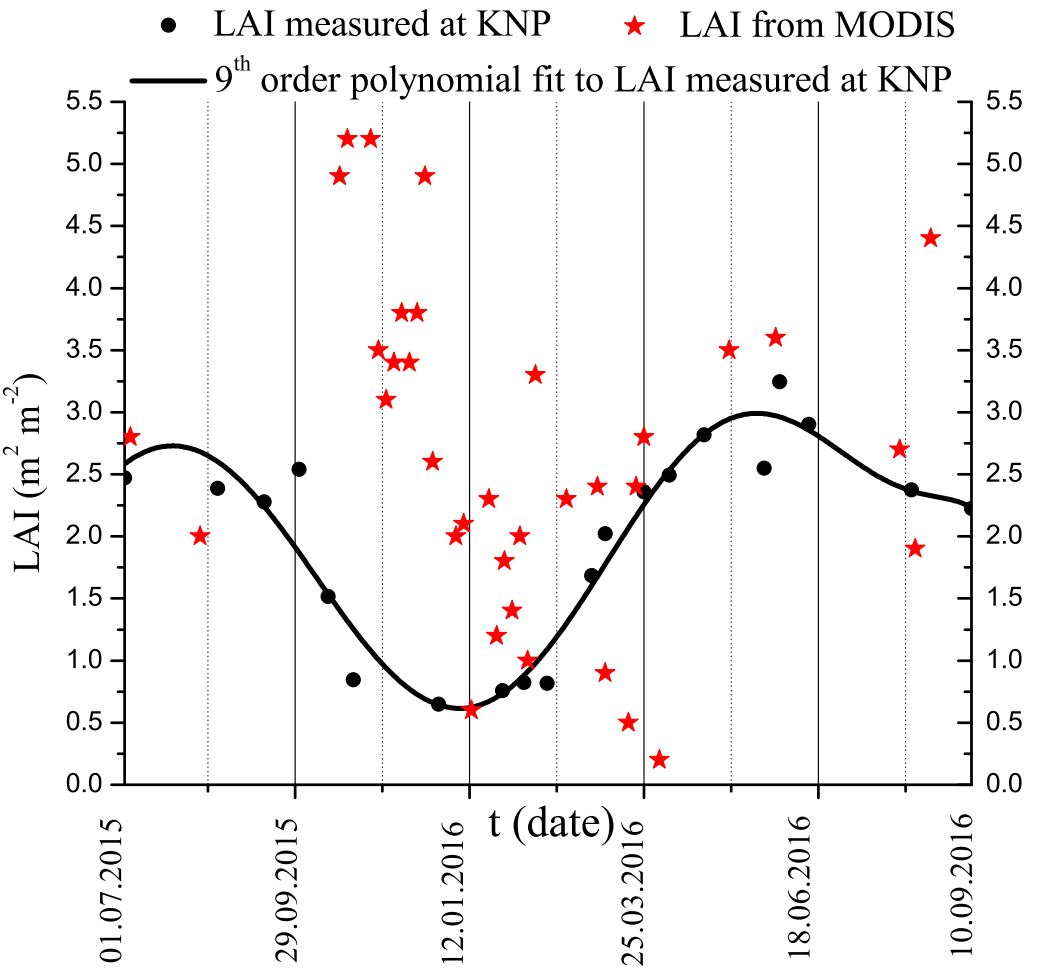

Figure 5: Measured, MODIS-derived and fit LAI during 01^{st} July, 2015 to 10^{th} September, 2016.

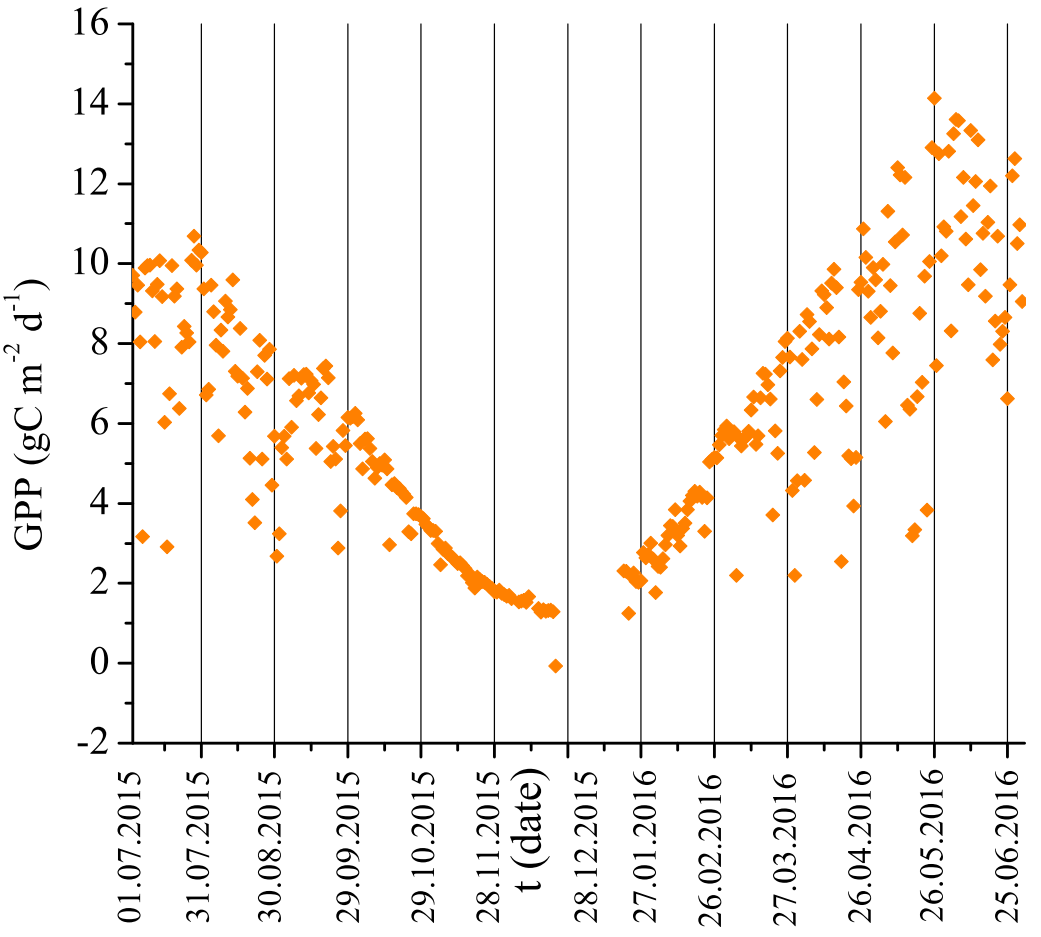

Figure 6: Modelled daily GPP using ACM during 01^{st} July, 2015 to 30^{th} June, 2016.

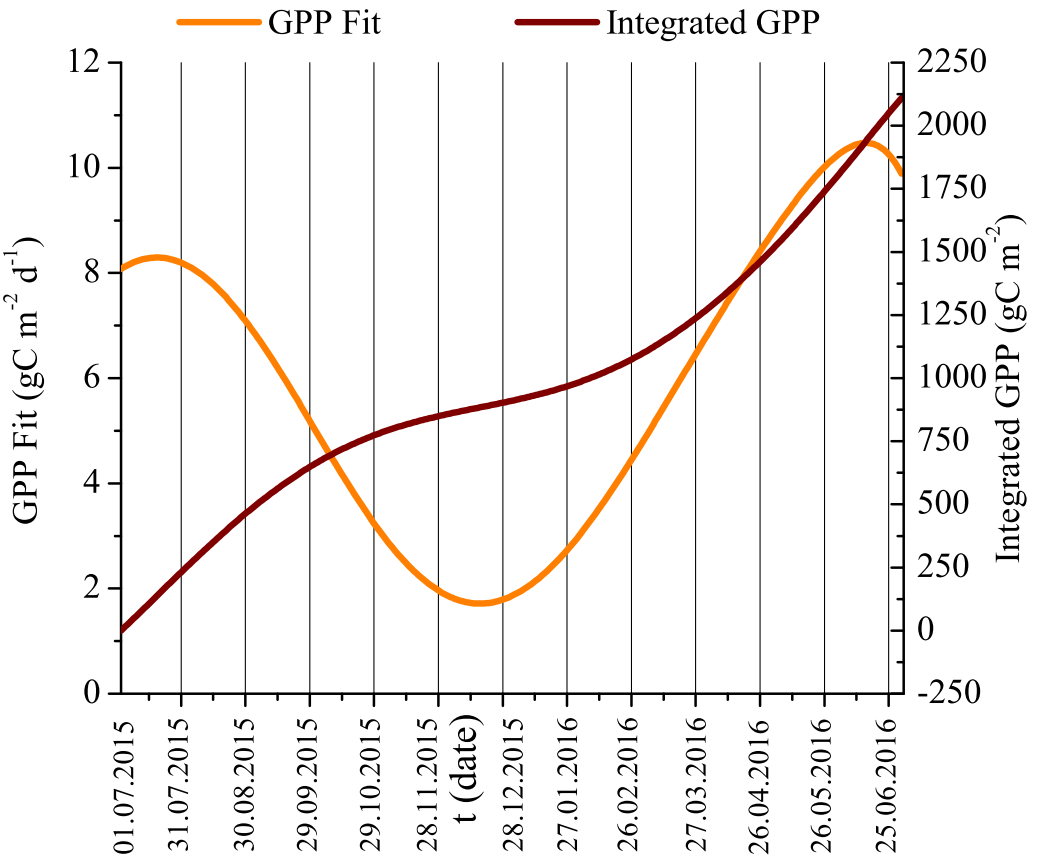

Figure 7: Polynomial fit to the modelled daily GPP and annual GPP calculated by integrating the fit during 01^{st} July, 2015 to 30^{th} June, 2016.